Published in final edited form as:
J Comp Neurol. 2011 February 1; 519(2): 341–357. doi:10.1002/cne.22522.

A Mosaic of Synaptic Contacts among Three Retinal Neurons

Amane Koizumi[*], **Tatjana C. Jakobs**[*], and **Richard H. Masland**
The Massachusetts Eye and Ear Infirmary, Harvard Medical School, Boston, MA 02114

Abstract

Retinal bipolar, amacrine and ganglion cells contact each other within precisely defined synaptic laminae, but the spatial distribution of contacts between the cells is generally treated as random. Here, we show that not to be the case. Excitatory inputs to inner retinal neurons were visualized by introduction of a plasmid coding for the postsynaptic protein PSD95-GFP. Our initial finding was that synapses upon the dendrites of retinal ganglion cells are regularly spaced, at 2–3 μm intervals, along the dendrites. Thus, the presence of a PSD95 punctum creates a nearby zone from which other inputs appear to be excluded. Despite their great variation in size and different morphologies, the spacing is similar for the arbors of different retinal ganglion cell types. Regular spacing was also observed for the starburst amacrine cells. This regularity is mirrored in the spacing of axonal varicosities of the stratified bipolar cells, which have a regular, non-random interval consistent with that of the PSD95 puncta upon ganglion cells. Thus, for each level of the inner plexiform layer, all three cell types participate in a single two-dimensional mosaic of synaptic contacts. These findings raise a new set of questions: How does the self-avoidance of synaptic sites along an individual dendrite arise and how is it physically maintained? Why is a regular spacing of inputs important for the computational function of the cells? Finally, which of the three players, if any, is developmentally responsible for the initial establishment of the pattern?

Keywords

retina; synapse; spacing; mosaic

Introduction

The neurons of the retina are not distributed randomly across the surface of the retina. Instead, cells of the same functional and morphological type keep a minimum distance from each other and the resulting "exclusion zone" leads to a regular mosaic of cells of the same type (Wässle et al., 1981; Reese and Galli-Resta, 2002). For ganglion cells, the dendritic arbors of neighboring cells of the same functional type overlap only minimally – thus, they tile the retina with a mosaic of cells. As there are at least a dozen different functional and morphological types of ganglion cells, there are more than twelve such mosaics, regular in themselves but completely independent of each other (Rockhill et al., 2000; Roska and Werblin, 2001; Rockhill et al., 2002). The physiological significance of this pattern is easy to understand; a random distribution of cells creates a pattern of clumps and gaps that would leave some parts of the retina oversampled, while other regions would be uncovered by cells of one particular type. Clumps in the mosaic represent redundancy, while gaps would create blind spots for the stimulus feature to which the cell type responds. A similar tiling exists for

For correspondence: Tatjana C. Jakobs, Howe Laboratory, 5th Floor, Massachusetts Eye and Ear Infirmary, 243 Charles Street, Boston, MA 02114, Tel. 617 391, Fax. 617 391 5938, tatjana_jakobs@meei.harvard.edu.
[*]The first two authors contributed equally to this work.

the coverage of body surfaces by somatosensory neurons (Nicholls and Baylor, 1968; Blackshaw et al., 1982; Grueber et al., 2001; Grueber et al., 2002; Jan and Jan, 2003).

We report here an analogous phenomenon that exists on the scale of individual synapses – a scale fine enough that the biological utility of the regularity is not immediately evident. The finding originated from a study directed toward a different goal. We wanted to know whether different functional types of ganglion cells have characteristically different patterns of synaptic input (Jakobs et al., 2008). To identify synaptic sites on the non-spiny dendrites of retinal ganglion cells, we used particle-mediated transfer of GFP-tagged PSD95 into cells in the ganglion cell layer of the rabbit retina. The tissue was then cultured to allow the expression of PSD95-GFP, which permits direct visualization of the excitatory synaptic sites of a single cell (Koizumi et al., 2007).

We found the overall density of excitatory input sites upon ganglion cells to be not notably different between cell types (Jakobs et al., 2008). What was not anticipated was that excitatory synaptic inputs onto the dendrites of retinal ganglion cells observe a minimum distance from each other, leading to a regular spacing along the length of the dendrite. In more formal terms, the positions of synapses are negatively autocorrelated, so that the occurrence of a synapse decreases the probability that another one lies nearby.

The spacing of synapses in other types of neuron has previously been studied. A well-studied example is the very regular mosaicism observed in fish retina, both the outer (Engström, 1963; Wagner, 1976) and the inner layers (Hibbard, 1971; Van Haesendonck and Missotten, 1983). The regular spacing in fish retina is observed on the level of cell bodies, as it is in mammalian retinas, but also for elements within the inner plexiform layer. Regular cell mosaics have been reported for amacrine and ganglion cell dendritic arbors and cell bodies (Podugolnikova, 1985a; Cook et al., 1992). The IPL of many fish is made up of ~25 sublayers, several of which contain highly regular lattices of bipolar axon terminals (Podugolnikova, 1985b) that are filled with glutamatergic vesicles (Van Haesendonck and Missotten, 1991). Interestingly, the mosaics formed by the axon terminals are even more regular in spacing than the bodies of the cells to which they belong (Mack, 2007). Although the postsynaptic elements have not been studied in detail, a high degree of regularity would be predicted for them as well.

The spatial distribution of axonal swellings in hippocampal neurons on a local scale is random, in that there is no significant exclusion zone around individual varicosities. Interestingly, however, the mean spacing across longer distances is deterministic, in the sense that an individual axon has the mean spacing characteristic for that type of axon and even for differing locations along its length (Shepherd et al., 2002; Shepherd and Raastad, 2003). A different kind of spatial ordering is observed for presynaptic active zones in the photoreceptors and neuromuscular junctions of flies. Within the photoreceptor terminals, synapses are regularly spaced, such that the presence of a synapse decreases the probability that another synapse lies nearby. In the neuromuscular junctions, each terminal varicosity has 15–40 synapses and these were again regularly spaced. This form of regular spacing suggests the presence of a physical interaction between nearby synapses within the terminals, perhaps initially during development (Meinertzhagen and Hu, 1996; Meinertzhagen et al., 1998; Dickman et al., 2006).

In our experiments, regularity of ganglion cell postsynaptic sites turned out to be a robust principle, observed for every ganglion cell type studied. In retrospect, it can also be seen in images of retinal neurons published in other contexts (Morgan et al., 2008; Xu et al., 2008). This is analogous in some ways to the tiling of the retinal surface by ganglion cell types. However, mosaics of synapses are a more complex case, as regularly spaced postsynaptic

sites require regular spacing of their presynaptic partners as well. The challenge of the present study was thus to understand the three dimensional arrangement of synapses among the interlocking cell populations of the inner retina.

Materials and Methods

Tissue preparation

New Zealand white rabbits of either sex aged 7–10 weeks were used for all experiments according to a protocol approved by the Committee for Animal Care of the Massachusetts Eye and Ear Infirmary. The retinas were removed and transfected with an expression plasmid encoding a fusion protein from PSD95 and GFP via particle-mediated gene transfer (Lo et al., 1994). The retinas were then cultured for four days in an organotypic retinal tissue culture. These methods are described in detail elsewhere (Koizumi et al., 2007; Jakobs et al., 2008). After four days of incubation, retinal tissue was mounted in glycerol and individual cells were chosen for image acquisition with a confocal microscope.

Ganglion cell types

Our sample included cells of six functional types (local edge detector (G1), small bistratified cell (G3), ON/OFF DS cell (G7), ON DS cell (G10), OFF-parasol cell (G5), and alpha cell (G11)), where the functional type had been correlated to a characteristic cell morphology in earlier studies (Barlow and Levick, 1965; Levick, 1967; Amthor et al., 1989a; Amthor et al., 1989b; Famiglietti, 1992; Dacey, 1993; Calkins et al., 1998; He and Masland, 1998; Roska and Werblin, 2001; Rockhill et al., 2002; Roska et al., 2006). The ganglion cells in our sample have been described and images presented in an earlier publication (Jakobs et al., 2008). Starburst cells were analyzed specifically for this study.

Statistical analysis

The cells were digitized using the Neurolucida package (Microbrightfield, Williston, VT). The skeleton of the dendritic arbor was entered, together with the location of PSD95 puncta and branch points. Cells digitized in this way are shown in Figures 1B, 3B and 7. For quantitative analysis of dendritic structure, the Neurolucida software package (Microbrightfield, Williston, VT) was used to trace individual ganglion cells from confocal image stacks in three dimensions. When the 3D stick figure of the cell's morphology was completed, markers were placed on PSD95 puncta and attached to the cell trace to identify the location of PSD95 puncta. The spatial resolution for each PSD95 punctum was 0.5 μm, because that was the limiting resolution of the confocal images.

Intervals between puncta were measured as illustrated in Figure 2. In general, measurements of synapse spacing were made along the dendrites, i.e. distances were measured along the extent of the dendrite. The exception was the spacing of varicosities of bipolar cell axons, which were measured from a stained field of cells or from individual cells, as described below; and these measurements were made in the conventional way (Wässle and Riemann, 1978; Rodieck, 1991), i.e. the spacing between varicosities was measured without reference to whether or not they lay on the axon of a particular cell. As a test of regularity for the intervals, they were compared with a model cell having the same number of PSD95 puncta placed at random by the uniform random generator of MatLab (The MathWorks, Natick, MA) on that dendritic arbor. The bin size for the random distributions was 0.5 μm. Possible differences between the interval distributions of real or randomized positions were statistically analyzed by the nonparametric 2 sample Kolmogorov-Smirnov test (Chakrarvarti et al., 1967; Rodieck, 1991) in Igor Pro (WaveMetrics, Lake Oswego, OR).

Nearest neighbor distances along the dendrites were analyzed using loglogistic fits of the distributions. Because it is constrained to a bounded space – essentially a line – the distribution of nearest neighbors along a dendrite was not fitted well with the usual Gaussian or Poisson distribution (chi-square test, $P < 0.1$). We evaluated exponential, Weibull, lognormal, and loglogistic curves. According to the chi-square goodness of fit test, the loglogistic curve fitted our data best. Curve fitting was done with the loglogistic probability density function shown below, by user written procedures in Igor Pro.

$$\text{Loglogistic probability density function}(x) = \frac{e^{\frac{\ln(x)-\mu}{\sigma}}}{\sigma \cdot x\left(1+e^{\frac{\ln(x)-\mu}{\sigma}}\right)^2} \quad (x>0)$$

with location parameter μ ($\mu > 0$) and scale parameter σ ($0 < \sigma < 1$).

Possible differences between the nearest neighbor distributions of real or randomized positions were statistically analyzed by the 2 sample Kolmogorov-Smirnov test.

The spatial autocorrelation (Density Recovery Profile, (Rodieck, 1991)) was measured within dendritic segments (Figure 2). Each punctum was considered once as the reference point. The distance from that punctum to all other puncta within its dendritic segment (i.e. between branch points) was measured. (Allowing the analysis to cross branch points gives the same fundamental result – the same exclusion zone – but incorporates much meaningless data from the hundreds of possible long paths that lead through distant parts of the cell's total dendritic arbor.) The inter-punctal distances were binned at 0.5 µm. If the dendritic segment had just one punctum, a DRP within that segment could not be measured. The density (puncta / linear µm) of puncta at any distance from the reference punctum was calculated as follows:

$$\text{Density (bin \#i)} = \frac{\sum_{j=1}^{N\ ref} \text{N puncta (ref \#j)(bin \#i)}}{S \cdot \sum_{j=1}^{N\ ref} \text{N dendrite(ref \#j)(bin \#i)}}$$

Where N ref = the number of reference puncta, N puncta (ref #j)(bin #i) = the number of puncta in bin #i from the reference punctum #j, S = bin size (0.5 µm), and N dendrite(ref #j) (bin #i) = the number of dendritic segments from the reference punctum #j that contain bin #i.

In this expression the average density is calculated as total number of reference puncta divided by the total length of the dendritic segments that have two or more of reference puncta. This is to allow for the varying length of the segments. It has the units puncta/ linear µm.

The distribution of PSD95 puncta around branch points was measured in a similar way. We calculated the distance from every branch point to all possible PSD95 puncta located on adjacent dendritic segments. The density (puncta / linear µm) was calculated as follows:

$$\text{Density (bin \#i)} = \frac{\sum_{j=1}^{N} \text{N puncta (branch point \#j) (bin \#i)}}{S \cdot \sum_{j=1}^{N} \text{N branch (branch point \#j)(bin \#i)}}$$

Where N = total number of branch points, N puncta (branch point #j)(bin #i) = the number of puncta in bin #i from the branch point #j, S = bin size (0.5 μm), and N branch (branch point #j)(bin #i) = the number of branches from the branch point #j that contain bin #i.

In all cases where the observed distributions were compared with random spacing, the randomly spaced data were fitted by an unsmoothed Gaussian. The distribution has a characteristically pointed shape because intervals smaller than 0.5 μm were not permitted in generating the random spacing.

The spacing of axonal varicosities in bipolar cells

The spatial distribution of axonal varicosites of bipolar cells was analyzed by nearest neighbor analysis (Wässle and Riemann, 1978). Immunostained terminal varicosities (CD15 cells) were analyzed as single fields sized 204 × 204 μm (Figure 4).

A different way to measure the spacing of varicosities of bipolar cells was to measure the spacing of varicosities in single-stained bipolar cells. As discussed later (Results) the nearest neighbor spacing of varicosities on single bipolar cells is a valid index of the population spacing because cone bipolar cells tile the retina: there is little or no overlap between neighbors. Thus many bipolar cells – as long as they are of the same type and are narrowly stratified – can be combined for analysis of the population statistics, i.e. the distribution of nearest neighbor distances. The bipolar cells studied here were from the set of stained cells collected by MacNeil et al. (MacNeil et al., 2004) and classified by them. Nearest neighbor distances were measured by conventional methods for the field of varicosities belonging to individual Golgi-stained cells of a single type, as shown in Table 3. The distributions of nearest neighbor distances were well fitted by Gaussian curves. Varicosities of the bipolar cells were also analyzed after staining of those cells as a population in retinal whole mounts using antibodies against the carbohydrate epitope CD15 (Brown and Masland, 1999).

Antibody characterization

Please see Table 1 for a list of all antibodies used. A monoclonal mouse IgM anti-CD15 antibody was used to stain for the population of $CD15^+$ bipolar cells (Brown and Masland, 1999). We have tested previously that preincubation of the tissue with synthetic CD15 epitope (Lacto-N-fucopentatose III, Sigma) completely blocks antibody staining in retinal tissue (Jakobs et al., 2003).

Calbindin immunoreactivity characterizes a type of bipolar cell in the rabbit retina (Massey and Mills, 1996), that has been identified with the CBb5 type in more recent studies (MacNeil et al., 2004). The affinity-purified rabbit polyclonal antibody against calbindin D-28k recognizes a 28kD protein in mouse brain extracts (Millipore, product data sheet). In the retina it detects horizontal cell bodies and processes in addition to CBb5 bipolar cells (Massey and Mills, 1996).

The mouse monoclonal antibody against CtBP2 (RIBEYE) recognizes a 48 kD band in BC3H1 cell extracts (BD Biosciences product data sheet). CtBP2 is one component of the natural fusion protein RIBEYE that is the major structural protein of synaptic ribbons in

photoreceptors and bipolar cells (Schmitz et al., 2000). Since RIBEYE contains a unique A domain in addition to the C-terminal portion of the protein that is nearly identical to the transcriptional repressor CtBP2, the antibody recognizes a ~110/120 kD double band in retina extracts that corresponds to RIBEYE, in addition to the 48 kD band that corresponds to CtBP2 which is also expressed in low levels in the retina (Schmitz et al., 2000). This antibody has been used in several immunohistochemical studies in the retina (Hirano et al., 2007; Jakobs et al., 2008; Lin et al., 2008), and was also shown to label ribbons in electron microscopy (tom Dieck et al., 2005). Secondary antibodies were FITC- or rhodamine-labeled donkey anti-mouse IgM or donkey anti-rabbit Fab2 fragments obtained from Jackson Immunoresearch (West Grove, PA).

Immunohistochemistry and image acquisition

Rabbit retinas were whole mounted on filter paper and incubated in primary antibodies for 3 days, followed by over-night incubation in the appropriate secondary antibody. The tissue was mounted in Vectashield (Vector Laboratories, Burlingame, CA) and imaged the day after mounting. All images were acquired on a Zeiss Axioplan II equipped with a BioRad Radiance confocal system. Images were taken with a C-Neofluar 63x/1.4 water immersion objective. The images were imported into Adobe Photoshop CS2 (Adobe) to adjust brightness or contrast. No other image processing was carried out.

Modeling the effects of synapse spacing

Three-dimensional cell traces captured by the Neurolucida program package were imported into the NEURON simulator (Neuron version 5.7 was downloaded from http://neuron.duke.edu/, (Hines and Carnevale, 1997; Carnevale and Hines, 2006). The reconstructed cells preserved the three dimensional direction, dendritic thickness, and connectivity of the dendrites. We incorporated excitatory synaptic input sites (PSD95 puncta) on the dendrites of the cell. The default passive parameters were: passive membrane conductance ($g\_pas = 25\ \mu S/cm^2$), intracellular cytoplasmic resistance (Ra = 150 ohm-cm), and membrane capacitance ($Cm = 1\ \mu F/cm^2$) that were determined in retinal cultured neurons by previous patch-clamp recordings and NEURON simulations (Koizumi et al., 2004; Koizumi et al., 2005). These parameters were incorporated uniformly in the reconstructed cell. No active currents were incorporated.

Excitatory synaptic inputs were mathematically described as an alpha-function with a decaying time course (tau = 1 msec), an appropriate maximum conductance (go, 1 mS/cm^2 in Figure 5, 50 $\mu S/cm^2$ in Figure 6 and Figure 7) and an equilibrium potential (Estim: for excitatory synaptic inputs, Estim = 0 mV). We assumed all synapses to have the same properties. The membrane potential of the cell was set to be −70 mV. We applied stimulation on all or parts of these synaptic input sites and recorded the somatic potential changes, as described under results. Subsequent statistical analysis was done with user-written procedures in MatLab and Igor Pro.

Results

Synaptic inputs are regularly spaced along the dendrites of retinal ganglion cells

We transfected retinal ganglion cells in an *ex-vivo* tissue culture of rabbit retina with expression plasmids for GFP-tagged PSD95 to label excitatory synaptic sites on the dendritic arbors. High-resolution confocal image stacks were taken of 56 cells, 10 of which were digitized using the NeuroLucida program package. This resulted in a database of 3-dimensional representations of the dendritic arbors and the excitatory synaptic sites of these cells. Evidence that PSD95 expressed in this way accurately reflects the sites of glutamatergic input was given previously (Jakobs et al., 2008), and was demonstrated

independently by Morgan et al. (2008). A preliminary analysis of this dataset was presented in our earlier publication, and the unprocessed data – images of the cells – have been made available (supplemental material to Jakobs et al., 2008). Here we report a detailed analysis of the local spatial patterns of excitatory synaptic inputs to the ganglion cells.

The spacing of PSD95-GFP puncta gave the visual impression of regularity (Figure 1, see also Figure 7) and this was confirmed by several measures. First, the overall frequency of the intervals between puncta showed a disproportionate number of mid-sized intervals, with a mode at about 3 μm for all cell types (Figure 2). When the same number of puncta were assigned positions at random, the distribution of intervals was significantly broader: it had more short intervals between puncta and more very long ones. These correspond to the clumps and “lakes” that visually characterize random spatial distributions. The inter-synapse interval was basically independent of the overall size of the dendritic arbor or the length of the individual segments, even though the dendritic field diameters vary by more than a factor of five from the smallest cells to the largest cells (Table 2).

Commonly used measures of spatial regularity in two dimensional spatial arrays are the nearest neighbor distances (Wässle and Riemann, 1978) and the spatial autocorrelation (density recovery profile, (Rodieck, 1991); see Cook (1996) for review). The nearest neighbor distributions for PSD95-GFP puncta along the dendrites of retinal ganglion cells were calculated as the nearest neighbors in the one dimensional case, i.e. the nearest neighbor along the dendrite (Figure 2). The events that cause this deviation from randomness are clearly seen in the spatial autocorrelation function (density recovery profile, DRP), which displays the distance from each punctum, taken as the origin, to all of the other puncta on that dendritic segment (a segment is the region of dendrite that lies between two branch points). Surrounding each punctum, there is a zone from which other puncta appear to be excluded.

The size of the exclusion zone did not vary significantly when the puncta were deliberately over- or undercounted during digitization of the raw images (data not shown). This is because a very large over- or undersampling of the image is required to obscure the underlying regularity (See Rodieck (1991); Cook (1996).)

Regular spacing of excitatory inputs to starburst amacrine cells

In addition to ganglion cells, many of the transfected retinas also contained labeled ON starburst amacrine cells, whose cell bodies reside in the ganglion cell layer. Inspection of the images suggested that their synaptic sites are regularly spaced and this was confirmed by quantitative analysis (Figure 3). The frequency distribution of synaptic intervals was wider than that for ganglion cells, with a mean nearest neighbor distance of 6.07 μm (Table 2), but the most frequent (modal) distance of about 3.5 μm was similar to that for ganglion cells. (This suggests that starburst cells skip potential inputs more often than ganglion cells, so that the mean interval is closer to the mode for ganglion cells than for starburst cells – see Discussion.)

Branch points affect the synapses of adjoining dendritic space

We repeated the autocorrelation analysis, but this time used the branch points as the points of reference – we computed the distribution of PSD95-GFP puncta on the two dendritic segments adjacent to the branch point, taking the branch point as the origin. The results are clearest for the largest cells, because these provide a larger sample of branch points, but were consistent for all cell types: a branch point appears to act as though it were a spatial organizer. Excitatory synaptic inputs may or may not be present at the branch point, as indicated by the presence or absence of intervals near 0. For the small bistratified (G3) cells

and ON DS cells there was a tendency for inputs to avoid branch points, but for the others the frequency of puncta at the branch point was near that expected by chance. In all cases, the branch points were surrounded by a zone from which excitatory synaptic inputs tended to be excluded. This zone was essentially the same size (~2 μm) as the exclusion zone that separates puncta within a segment. In other words, whether there was an excitatory input at the branch point or not, it tended to set the start point for the series of regular intervals that divide up the dendritic segment.

The axonal varicosities of bipolar cells are also regularly spaced

The major excitatory input to retinal ganglion and amacrine cells comes from the axon terminals of bipolar cells. Like ganglion cells, these come in a variety of different types, distinguished primarily by their level of stratification within the inner plexiform layer (MacNeil et al., 2004; Wässle, 2004; Wässle et al., 2009). It seemed possible that regularities would be found in their axonal terminals as well: a given level of the inner plexiform layer is occupied by only a few types – in some cases a single type – of retinal ganglion cell. If that is the case, and if the ganglion and starburst cells have excitatory input zones spaced at ~3 μm, then a corresponding spacing would be expected on the presynaptic side. We therefore undertook to study the axonal varicosities – the sites where their ribbon synapses are located – of bipolar cells.

Two independent types of material were used. First, we stained the population of type CBb4 bipolar cells (MacNeil et al., 2004) in whole mounts using an antibody directed against the carbohydrate epitope CD15 (Brown and Masland, 1999). We carried out nearest neighbor analysis on the axonal swellings of these cells, which are the primary sites of their ribbon synapses (Figure 4AB). Because the whole population of cells was simultaneously stained, here we could use the standard two dimensional nearest neighbor analysis. We found that these varicosities were regularly spaced, with a mean nearest neighbor distance of 4.2 ± 0.1 μm (n= 3 fields).

Does this principle apply to other types of bipolar cell? If we had ways to stain all of the bipolar cell types as whole populations, then we could have used standard NND or DRP analysis of the fields of stained axonal varicosities, as for the CD15 cells. For most bipolar cell types, we did not have such a staining capability. We realized, however, that the characteristics of bipolar cell axonal arbors allow testing the hypothesis by a different method, in which the spacing of synapses on individual cells is examined and from this the population spacing derived. The cells were Golgi-impregnated (Figure 4C) and have been described and classified in a previous study (MacNeil et al., 2004). It was possible to achieve an adequate sample for nearest neighbor analysis because nearest neighbor analysis depends only upon the single nearest neighbor to the reference varicosity; in contrast to DRP analysis, it ignores any members of the population more distant than the nearest neighbor. As long as the processes of neighboring cells do not overlap substantially, the nearest neighbor will virtually always be from within the same cell – indeed, it is usually along the same dendrite – so that an approximation of the nearest neighbor distance of the whole population can be obtained from the nearest neighbors that occur within a series of its individual members; it is not necessary to stain the cells as a population. The necessary condition of non-overlap is met for cone bipolar cells, most of which have axonal coverage factors of unity or less (Mills and Massey, 1992; Milam et al., 1993; Brown and Masland, 1999; Lin and Masland, 2005).

We studied bipolar cells that terminate at four different depths; they arborized at approximately 20, 40, 55, and 75% depth of the inner plexiform layer. (The CD15 population arborized at 80%.) The results are illustrated for cells stratified at 0 to 20% of the

IPL in Figure 4B and detailed in Table 3. The spacing of varicosities was similar at all levels of the inner plexiform layer, with a mean nearest neighbor distance of 3.98 μm.

This is slightly wider than the spacing of postsynaptic sites along ganglion or amacrine cell dendrites, but the difference is within the experimental errors of measurement. The largest of these is the necessity to correct for shrinkage in the Golgi material, which was dehydrated and cleared: We applied the usual 30% correction, but there was no internal standard by which this value could be cross-checked. Another limitation is that axonal varicosities of bipolar cells, some of which are as much as 3 μm in extent, sometimes contain more than one ribbon synapse. We measured the frequency of occurrence of varicosities containing one, two or more synaptic ribbons in wholemounts double stained for calbindin, which marks the CBb5 type of bipolar cell, and RIBEYE (data not shown). Varicosities containing one or two ribbons were observed in the large majority (81%) of all cases. Multi-ribbon varicosities tended to be associated with extended PSD95 puncta but these were not distinguished in our mapping of postsynaptic sites, which made no distinction between large PSD95 puncta and small ones.

Regular spacing decreases the variability of an individual dendrite's response to small stimuli, but this has little effect in a structurally realistic cell

We next investigated the possible physiological consequences of regularly spaced inputs to the retinal ganglion cells. This was studied by biophysical modeling, comparing the behavior of a retinal ganglion cell that possesses regularly spaced inputs with the same cell having its inputs distributed at random positions. These studies utilized first a highly simplified retinal ganglion cell and then a more spatially realistic one.

We began by asking the extent to which the biophysical contributions of individual synaptic inputs are affected by neighboring ones. Do inputs to neighboring synapses sum linearly or non-linearly; and to what extent is this affected by the distance between them? We constructed a model cell that had only a single straight dendrite. As a starting point, this dendrite was assigned membrane properties obtained by double patch-clamp recording from dendrites of retinal neurons in culture (Koizumi et al., 2005). In the simulation, we injected current into individual synapses or pairs of synapses spaced at various distances; the response at the soma was recorded. In the range of PSD95 spacing observed in our data, we found virtually no interaction between neighboring inputs: the inputs summed linearly at all distances between pairs of inputs. This result held for all plausible values of the biophysical parameters assumed in the simulation (Figure 5).

A different question is how the spacing of synapses might, or might not, affect the transmission of information through the ganglion cell under various conditions of inputs. In this exercise we imagine the ganglion cell as a device that samples the output of a field of bipolar cells. We ask how reliably the ganglion cell can report the bipolar cell output when the ganglion cell's synaptic inputs have regular or random spacing. The simulated cell was assigned glutamatergic inputs at an average spacing of 3 μm, approximating that observed for synapses of the ganglion cells in our sample. To avoid distortion by chance variation in a single random drawing, quantitative comparisons were made using a series of random positions.

The first test case used the simplified cell that has only a single 250 μm dendrite (Figure 6). If the whole cell was stimulated, there was no difference in the soma response with random or regular spacing of the synapses. We considered the response of the cell to patches of inputs that covered a span of 27, 51 or 75 μm, a range similar to the diameters of the smallest bipolar cell axonal arbors in the rabbit (McGillem and Dacheux, 2001; MacNeil et al., 2004). All of the synapses covered by the stimulus were considered to be activated. The

response of the cell at the soma was measured. In all cases there was a gradual decrement as the input moved from near the soma to the distal end of the dendrite. When the spacing of synaptic inputs was random, the resulting irregularities caused variability in the somal output: this would increase the uncertainty with which this cell signals the presence of an input. (The timing of the responses was little affected, Figure 6, inset). The variance in the simulated response to a 27 μm bar was ~ fourfold greater for the randomly spaced inputs than for the regular spacing: s.d. = 0.64 mV; random spacing: s.d. = 2.64 mV (n=59). For the 51 μm stimulus the corresponding values were 1.38 and 2.93 mV (n=51) and for the 75 μm stimulus they were 1.88 mV and 2.57 mV (n=43).

Would the same thing happen in the case of the actual geometry of a ganglion cell? Such a simulation is shown in Figure 7. The cell was the same OFF parasol cell analyzed in Figure 2. In one case the synaptic input zones were assigned their actual positions as observed from PSD95 expression; in the other, the same number of synaptic zones was positioned throughout the dendritic arbor at random. Inputs of different spatial extent were applied throughout the dendritic arbor and the cell's response at the soma was calculated. At 50 μm there was little difference between the random input and the regular input case. At 25 μm there was somewhat more variability in output with random spacing of inputs than with regular. The largest effect was a slightly greater number of particularly effective locations (hot spots) in the random case (arrows). These are caused by clumps of inputs that occur when inputs are assigned at random positions. If such a clump occurs near the soma, where it efficiently drives the somatic membrane potential, a hot spot in stimulus effectiveness results. However, the difference between regular and random spacing is much less than in the reduced cell with only a single axon. This is because of the space-filling character of the dendritic arbor (Panico and Sterling, 1995): a test probe approximating the size of a bipolar axonal field usually falls upon more than one dendritic branch, and the averaging that this creates smoothes the final output of the model cell.

Discussion

The mosaic of excitatory synapses in the inner plexiform layer

In trying to conceptualize the mosaic of synapses, it is useful to begin by focusing on the array of axon terminals of any single type of narrowly stratified bipolar cell – a sheet of terminals like the one shown in Figure 4A. These arrays are themselves regular, both from cell to cell and within the varicosities of a single cell. This was measured quantitatively in the present study and is evident from simple inspection of many previously published images (Massey and Mills, 1996; Jacoby et al., 2000; Trexler et al., 2001; Zhang et al., 2002; Li et al., 2004; MacNeil et al., 2004). It seems to be a general pattern for many, if not all, types of bipolar cells – at least those that are narrowly stratified within the inner plexiform layer. In the present study, significantly non-random nearest neighbor distances were seen at four different depths within the IPL. Furthermore, all types of retinal ganglion cells had regularly spaced excitatory inputs along their dendrites, and those include ganglion cells that stratify at many different depths within the inner plexiform layer. Thus, regularly spaced mosaics are the rule for many, if not all, bipolar and ganglion cells.

Without imputing causality (see below), it is evident that the regular spacing of bipolar cell varicosities is associated with the appearance of the "exclusion zone" along the length of the ganglion cell dendrites: A ganglion cell dendrite that samples from a regularly spaced two dimensional mosaic of synaptic outputs necessarily has some degree of regularity in the positions of synaptic inputs along its dendrites. This is illustrated in Figure 8, a schematic representation of the present results. The fundamental mosaic of excitatory inputs is shown by the red dots, representing output sites (with one or more ribbon synapses) of the bipolar

varicosities. The ganglion cell (blue) and the amacrine cell (green) both sample from this mosaic.

Just as for the retinal mosaics of cell types, the exclusion of excitatory synapses from each others' neighborhood pertains to other synapses of the same type – to excitatory synapses but not to inhibitory ones. Inhibitory synapses (either glycinergic or GABAergic) make up approximately 80% of all synapses upon most retinal ganglion cell dendrites and are thus far more numerous than the excitatory inputs studied here (Stevens et al., 1980; Freed and Sterling, 1988; Macri et al., 2000; Jeon et al., 2002; Famiglietti, 2005). They clearly are permitted to lie within the exclusion zone of the excitatory inputs. This is in many ways analogous to the problem raised by tiling of the retinal surface by ganglion cells, which are evenly spaced with respect to other members of the same cell type, but are randomly spaced with respect to ganglion cells of other functional types.

How is the regular mosaic created?

It is easy to fall into conceptualizing the mosaic of inner retinal contacts as being organized developmentally around the mosaic of varicosities of the bipolar cells. The problem is that the bipolar cells are the last retinal neurons to be developmentally specified (Young, 1985); and their ribbon synapses are the last synapses to appear within the inner plexiform layer (McArdle et al., 1977). Therefore, at least two sequences of events should be considered, here described in simplified terms.

(1) Ganglion cell dendrites contain the signals that create regular spacing. Ganglion cells are the first retinal neurons to develop (Young, 1985), for review see Marquardt and Gruss (2002). They could contain a cell-intrinsic mechanism for creating regular spacing of their synaptic input sites. In the extreme case, the cell could "know" where each synapse should lie. More plausibly, a mechanism could exist – possibly in the cytoskeleton – that defines a minimal space between excitatory synapses. Since PSD95 is an intracellular protein, it would provide a recognition site. This would create the exclusion zone, with the eventual consequence of regular spacing of postsynaptic sites along the dendrite. In this scenario, the postsynaptic sites would attract input from the bipolar cells, so that the primary spacing event is the spacing of sites along the ganglion or starburst cell dendrites and the regular spacing of bipolar cell axon terminals is a secondary consequence.

(2) Bipolar cell endings are the original source of regular spacing. In this sequence the spacing of bipolar cell outputs is created first, and the postsynaptic specializations follow: the regular spacing of PSD95 puncta on ganglion and amacrine dendrites is induced by the spacing of the presynaptic elements. Bipolar cells taken as a whole repel other bipolar cells of the same type. Conceivably the same signals could cause self-repulsion of the branches of bipolar cell axons (Fuerst et al., 2008), resulting in the regular mosaic of bipolar cell axon terminals. The presynaptic elements of bipolar to ganglion synapses would induce PSD95 aggregates in the ganglion cells, which would then be regularly spaced because the bipolar cell synapses are regularly spaced. This would require that the formation of postsynaptic elements be delayed in retinal ganglion and amacrine cells until after bipolar ribbons are present, or that the site of the future synapse be molecularly defined before the ribbons appear, or that preformed postsynaptic sites are directed to migrate by a signal from the bipolar cell synapses. The induction of acetylcholine receptor clusters by motor axons is a precedent for such an induction of postsynaptic specializations by afferent contacts.

This discussion ignores the presence of inhibitory synapses and these form the majority of synaptic inputs to retinal ganglion and amacrine cells. Conventional synapses of the rabbit retina appear in the inner plexiform layer before ribbon synapses (McArdle et al., 1977). At a coarse level, therefore, inhibitory synapses should be present before the excitatory ones

studied here. Little is known about the formation of the subtypes of inhibitory synapse; indeed, some are converted from an excitatory function to an inhibitory one during development (Ben-Ari, 2002; Zheng et al., 2004). The two possible mechanisms of spacing listed above would operate without influence from inhibitory inputs (just as the retinal mosaics of soma types are independent of each other) but this is an assumption that awaits direct test.

What is the biological utility of regular spacing?

A regular spacing of axonal varicosities is seen in unmyelinated axons in the hippocampus and cerebellum (Shepherd et al., 2002). However, there are many cases of neurons in which the spacing of excitatory inputs appears much less orderly (see images 1 and 2 in Shepherd et al. (2002)). Furthermore, it is not necessary *a priori* that the PSD95 zones of retinal ganglion cells have the particular spacing that is observed: a 2.5–4 μm gap along the dendrite is physically wide enough to contain many additional PSD95 zones, and excitatory synapses with closer spacing are observed on the dendrites of other neurons of the central nervous system. Regular spacing of synaptic contacts in the inner plexiform layer does not exist out of mechanical necessity; it exists for a biological reason.

We hypothesized that regular spacing might exist in order to avoid over- or undersampling of visual space, by analogy with the mosaics of dendritic fields that cover the retinal surface. However, that does not seem to be the case. The reason is that the spacing of the synapses occurs on a finer scale than the axonal fields of bipolar cells, and it is those axonal fields that determine the spatial resolution of information transmitted from the photoreceptor mosaic to the inner retina.

We also simulated the effects of random or regular spacing on the physiological responses of simulated retinal ganglion cells. Simulated inputs were applied to the dendrites of ganglion cells, and the physiological responses of the cells were modeled. Random spacing of synaptic input sites did increase the variability of response of the cells, but the effect was not great; and it only occurred when the simulated area of input was smaller than that of a realistic axon terminal of a bipolar cell (Figures 5–6). Other biophysical speculations are possible. Spacing along the dendrite may be required because of the interplay between injection of synaptic currents and the other functional elements present in the microenvironment of the dendrite: inhibitory synaptic inputs, ion channel proteins, and second messenger systems. For example, regular spacing might be required to ensure uniform diffusion of Ca^{2+} or another biological messenger to structures around the excitatory synapse.

Finally, it is possible that regular spacing serves a quite different kind of need, that of architectural economy. An example is the proposed conservation of what has been termed “wire length” (Chklovskii et al., 2002; Klyachko and Stevens, 2003; Song et al., 2005; Chen et al., 2006). The retina – more than almost any other CNS structure – is under enormous constraints of size, since the packing density of its elements translates directly into the spatial acuity of vision. The inner plexiform layer, about 20 μm thick in the rabbit, contains processes of more than 50 functionally distinct types of neurons, each of which must find its correct partners. Perhaps regular spacing helps solve this complex geometric problem, creating a matrix around which connectivity can be organized with efficiency.

Overview: the organization of excitatory inputs onto mammalian retinal ganglion cells—This study and our previous one (Jakobs et al., 2008) reveal a distribution of excitatory inputs to ganglion cells simpler than would have been anticipated from the textbook picture of dendritic integration. That view is derived primarily from brain neurons, where patterns of excitation, inhibition and branching can for purely electrotonic reasons

create non-linearities in the input-output relations of the dendrites (for review, see Shepherd (2003).) We see no evidence of the specializations that would support such complexities in the excitatory inputs to retinal ganglion cells. The reason is quite likely a simple matter of size. Retinal ganglion cells are, by the standards of projection neurons in the brain, tiny cells. Their longest dendrites are on average more than an order of magnitude shorter than those of hippocampal or neocortical pyramidal cells. Given plausible length constants, dendrites this short have far less opportunity for electrotonic integration based on dendritic geometry.

Indeed, the distribution and spacing of retinal ganglion cell inputs are consistent with a view in which the ganglion cell is electrotonically compact, simply summing its inputs. The same pattern of excitatory inputs and spacing is observed across our whole sample, despite the ganglion cells' manifest differences in receptive field size, dendritic field size, branching pattern, levels of stratification, and tuning to the visual stimulus. The dominant feature of this pattern is its uniformity, of both synapse spacing and spatial distribution, across all parts of the dendritic arbor and all types of retinal ganglion cell.

This is not to say that dendritic integration does not occur in retinal ganglion cells. Another difference from the brain neurons is that the inner retinal neurons receive a much higher ratio of inhibitory to excitatory input (Megias et al., 2001) and this richness of inhibition (Taylor et al., 2000; Roska and Werblin, 2001; Van Wyk et al., 2006; Sivyer et al., 2010) can create complexity in the reponses of the cells. Visual inspection of published images indicates that inhibitory inputs are also distributed throughout the dendritic arbors of retinal ganglion cells, but these inputs come from a variegated collection of amacrine cells and can convey very different properties to the ganglion cells (Roska and Werblin, 2001; Werblin et al., 2001). Perhaps these massive inhibitory inputs substitute for the passive integration seen in larger projection neurons. Finally, and most importantly, the active properties of the dendrites create major non-linearities, and these are clearly demonstrated to play a large role in the physiology of the dendrites: a vivid example is the role of dendritic spikes in the creation of directionally selective responses (Taylor et al., 2000; Euler et al., 2002; Oesch et al., 2005). This is almost certainly elaborated in other ways in other types of ganglion cells, each of which expresses a distinct signature of conductances (O'Brien et al., 2002). We imagine the regularly distributed excitatory inputs of retinal ganglion cells as a foundation – a fundamental canvas upon which the more complex physiologies of the dendrites are painted.

Acknowledgments

We thank Yixin Ben and Ming Lye-Barthel for technical assistance and Bingxing Huo for drawing Figure 8.

Funded by: NIH grants RO1 017169 and RO1 EY019703. RHM is a Senior Investigator of Research to Prevent Blindness

References

Amthor FR, Takahashi ES, Oyster CW. Morphologies of rabbit retinal ganglion cells with complex receptive fields. J Comp Neurol. 1989a; 280(1):97–121. [PubMed: 2918098]

Amthor FR, Takahashi ES, Oyster CW. Morphologies of rabbit retinal ganglion cells with concentric receptive fields. J Comp Neurol. 1989b; 280(1):72–96. [PubMed: 2918097]

Barlow H, Levick W. The mechanism of directionally selective units in rabbit`s retina. J Physiol. 1965; 178:477–504. [PubMed: 5827909]

Ben-Ari Y. Excitatory actions of gaba during development: the nature of the nurture. Nat Rev Neurosci. 2002; 3(9):728–739. [PubMed: 12209121]

Blackshaw SE, Nicholls JG, Parnas I. Physiological responses, receptive fields and terminal arborizations of nociceptive cells in the leech. J Physiol. 1982; 326:251–260. [PubMed: 7108790]

Brown SP, Masland RH. Costratification of a population of bipolar cells with the direction-selective circuitry of the rabbit retina. J Comp Neurol. 1999; 408(1):97–106. [PubMed: 10331582]

Calkins DJ, Tsukamoto Y, Sterling P. Microcircuitry and mosaic of a blue-yellow ganglion cell in the primate retina. J Neurosci. 1998; 18(9):3373–3385. [PubMed: 9547245]

Carnevale, NT.; Hines, ML. The NEURON book. Cambridge, UK: Cambridge University Press; 2006.

Chakrarvarti, IM.; Laha, RG.; Roy, J. Handbook of Methods of Applied Statistics. New York: John Wiley & Sons; 1967.

Chen BL, Hall DH, Chklovskii DB. Wiring optimization can relate neuronal structure and function. Proc Natl Acad Sci U S A. 2006; 103(12):4723–4728. [PubMed: 16537428]

Chklovskii DB, Schikorski T, Stevens CF. Wiring optimization in cortical circuits. Neuron. 2002; 34(3):341–347. [PubMed: 11988166]

Cook JE. Spatial properties of retinal mosaics: an empirical evaluation of some existing measures. Vis Neurosci. 1996; 13(1):15–30. [PubMed: 8730986]

Cook JE, Becker DL, Kapila R. Independent mosaics of large inner- and outer-stratified ganglion cells in the goldfish retina. J Comp Neurol. 1992; 318(4):355–366. [PubMed: 1578007]

Dacey DM. Morphology of a small-field bistratified ganglion cell type in the macaque and human retina. Vis Neurosci. 1993; 10(6):1081–1098. [PubMed: 8257665]

Dickman DK, Lu Z, Meinertzhagen IA, Schwarz TL. Altered synaptic development and active zone spacing in endocytosis mutants. Curr Biol. 2006; 16(6):591–598. [PubMed: 16546084]

Engström K. Cone types and cone arrangements in teleost retinae. Acta Zool. 1963; 44:179–243.

Euler T, Detwiler PB, Denk W. Directionally selective calcium signals in dendrites of starburst amacrine cells. Nature. 2002; 418(6900):845–852. [PubMed: 12192402]

Famiglietti EV. Dendritic co-stratification of ON and ON-OFF directionally selective ganglion cells with starburst amacrine cells in rabbit retina. J Comp Neurol. 1992; 324(3):322–335. [PubMed: 1383291]

Famiglietti EV. Synaptic organization of complex ganglion cells in rabbit retina: type and arrangement of inputs to directionally selective and local-edge-detector cells. J Comp Neurol. 2005; 484(4): 357–391. [PubMed: 15770656]

Freed MA, Sterling P. The ON-alpha ganglion cell of the cat retina and its presynaptic cell types. J Neurosci. 1988; 8(7):2303–2320. [PubMed: 3249227]

Fuerst PG, Koizumi A, Masland RH, Burgess RW. Neurite arborization and mosaic spacing in the mouse retina require DSCAM. Nature. 2008; 451(7177):470–474. [PubMed: 18216855]

Grueber WB, Graubard K, Truman JW. Tiling of the body wall by multidendritic sensory neurons in Manduca sexta. J Comp Neurol. 2001; 440(3):271–283. [PubMed: 11745623]

Grueber WB, Jan LY, Jan YN. Tiling of the Drosophila epidermis by multidendritic sensory neurons. Development. 2002; 129(12):2867–2878. [PubMed: 12050135]

He S, Masland RH. ON direction-selective ganglion cells in the rabbit retina: dendritic morphology and pattern of fasciculation. Vis Neurosci. 1998; 15(2):369–375. [PubMed: 9605536]

Hibbard E. Grid patterns in the retinal organization of the cichlid fish Astronotus ocellatus. Exp Eye Res. 1971; 12(2):175–180. [PubMed: 5119351]

Hines ML, Carnevale NT. The NEURON simulation environment. Neural Comput. 1997; 9(6):1179–1209. [PubMed: 9248061]

Hirano AA, Brandstatter JH, Vila A, Brecha NC. Robust syntaxin-4 immunoreactivity in mammalian horizontal cell processes. Vis Neurosci. 2007; 24(4):489–502. [PubMed: 17640443]

Jacoby RA, Wiechmann AF, Amara SG, Leighton BH, Marshak DW. Diffuse bipolar cells provide input to OFF parasol ganglion cells in the macaque retina. J Comp Neurol. 2000; 416(1):6–18. [PubMed: 10578099]

Jakobs TC, Ben Y, Masland RH. CD15 immunoreactive amacrine cells in the mouse retina. J Comp Neurol. 2003; 465(3):361–371. [PubMed: 12966561]

Jakobs TC, Koizumi A, Masland RH. The spatial distribution of glutamatergic inputs to dendrites of retinal ganglion cells. J Comp Neurol. 2008; 510(2):221–236. [PubMed: 18623177]

Jan YN, Jan LY. The control of dendrite development. Neuron. 2003; 40(2):229–242. [PubMed: 14556706]

Jeon CJ, Kong JH, Strettoi E, Rockhill R, Stasheff SF, Masland RH. Pattern of synaptic excitation and inhibition upon direction-selective retinal ganglion cells. J Comp Neurol. 2002; 449(2):195–205. [PubMed: 12115689]

Klyachko VA, Stevens CF. Connectivity optimization and the positioning of cortical areas. Proc Natl Acad Sci U S A. 2003; 100(13):7937–7941. [PubMed: 12796510]

Koizumi A, Hayashida Y, Kiuchi T, Yamada Y, Fujii A, Yagi T, Kaneko A. The interdependence and independence of amacrine cell dendrites: patch-clamp recordings and simulation studies on cultured GABAergic amacrine cells. J Integr Neurosci. 2005; 4(3):363–380. [PubMed: 16178063]

Koizumi A, Jakobs TC, Masland RH. Inward rectifying currents stabilize the membrane potential in dendrites of mouse amacrine cells: patch-clamp recordings and single-cell RT-PCR. Mol Vis. 2004; 10:328–340. [PubMed: 15152185]

Koizumi A, Zeck G, Ben Y, Masland RH, Jakobs TC. Organotypic culture of physiologically functional adult Mammalian retinas. PLoS ONE. 2007; 2:e221. [PubMed: 17311097]

Levick WR. Receptive fields and trigger features of ganglion cells in the visual streak of the rabbits retina. J Physiol. 1967; 188(3):285–307. [PubMed: 6032202]

Li W, Keung JW, Massey SC. Direct synaptic connections between rods and OFF cone bipolar cells in the rabbit retina. J Comp Neurol. 2004; 474(1):1–12. [PubMed: 15156575]

Lin B, Masland RH. Synaptic contacts between an identified type of ON cone bipolar cell and ganglion cells in the mouse retina. Eur J Neurosci. 2005; 21(5):1257–1270. [PubMed: 15813935]

Lin B, Masland RH, Strettoi E. Remodeling of cone photoreceptor cells after rod degeneration in rd mice. Exp Eye Res. 2008

Lo DC, McAllister AK, Katz LC. Neuronal transfection in brain slices using particle-mediated gene transfer. Neuron. 1994; 13(6):1263–1268. [PubMed: 7993619]

Mack AF. Evidence for a columnar organization of cones, Muller cells, and neurons in the retina of a cichlid fish. Neuroscience. 2007; 144(3):1004–1014. [PubMed: 17156929]

MacNeil MA, Heussy JK, Dacheux RF, Raviola E, Masland RH. The population of bipolar cells in the rabbit retina. J Comp Neurol. 2004; 472(1):73–86. [PubMed: 15024753]

Macri J, Martin PR, Grünert U. Distribution of the alpha1 subunit of the GABA(A) receptor on midget and parasol ganglion cells in the retina of the common marmoset Callithrix jacchus. Vis Neurosci. 2000; 17(3):437–448. [PubMed: 10910110]

Marquardt T, Gruss P. Generating neuronal diversity in the retina: one for nearly all. Trends Neurosci. 2002; 25(1):32–38. [PubMed: 11801336]

Massey SC, Mills SL. A calbindin-immunoreactive cone bipolar cell type in the rabbit retina. J Comp Neurol. 1996; 366(1):15–33. [PubMed: 8866843]

McArdle CB, Dowling JE, Masland RH. Development of outer segments and synapses in the rabbit retina. J Comp Neurol. 1977; 175(3):253–274. [PubMed: 903423]

McGillem GS, Dacheux RF. Rabbit cone bipolar cells: correlation of their morphologies with whole-cell recordings. Vis Neurosci. 2001; 18(5):675–685. [PubMed: 11925003]

Megias M, Emri Z, Freund TF, Gulyas AI. Total number and distribution of inhibitory and excitatory synapses on hippocampal CA1 pyramidal cells. Neuroscience. 2001; 102(3):527–540. [PubMed: 11226691]

Meinertzhagen IA, Govind CK, Stewart BA, Carter JM, Atwood HL. Regulated spacing of synapses and presynaptic active zones at larval neuromuscular junctions in different genotypes of the flies Drosophila and Sarcophaga. J Comp Neurol. 1998; 393(4):482–492. [PubMed: 9550153]

Meinertzhagen IA, Hu X. Evidence for site selection during synaptogenesis: the surface distribution of synaptic sites in photoreceptor terminals of the files Musca and Drosophila. Cell Mol Neurobiol. 1996; 16(6):677–698. [PubMed: 9013030]

Milam AH, Dacey DM, Dizhoor AM. Recoverin immunoreactivity in mammalian cone bipolar cells. Vis Neurosci. 1993; 10(1):1–12. [PubMed: 8424920]

Mills SL, Massey SC. Morphology of bipolar cells labeled by DAPI in the rabbit retina. J Comp Neurol. 1992; 321(1):133–149. [PubMed: 1613135]

Morgan JL, Schubert T, Wong RO. Developmental patterning of glutamatergic synapses onto retinal ganglion cells. Neural Develop. 2008; 3:8.

Nicholls JG, Baylor DA. Specific modalities and receptive fields of sensory neurons in CNS of the leech. J Neurophysiol. 1968; 31(5):740–756. [PubMed: 5711143]

O'Brien BJ, Isayama T, Richardson R, Berson DM. Intrinsic physiological properties of cat retinal ganglion cells. J Physiol. 2002; 538(Pt 3):787–802. [PubMed: 11826165]

Oesch N, Euler T, Taylor WR. Direction-selective dendritic action potentials in rabbit retina. Neuron. 2005; 47(5):739–750. [PubMed: 16129402]

Panico J, Sterling P. Retinal neurons and vessels are not fractal but space-filling. J Comp Neurol. 1995; 361(3):479–490. [PubMed: 8550894]

Podugolnikova TA. Inner plexiform layer of jack mackerel retina: participation of amacrine and ganglion cells in its spatial organization. Vision Res. 1985a; 25(12):1853–1864. [PubMed: 3832609]

Podugolnikova TA. Morphology of bipolar cells and their participation in spatial organization of the inner plexiform layer of jack mackerel retina. Vision Res. 1985b; 25(12):1843–1851. [PubMed: 3832608]

Reese BE, Galli-Resta L. The role of tangential dispersion in retinal mosaic formation. Prog Retin Eye Res. 2002; 21(2):153–168. [PubMed: 12062533]

Rockhill RL, Daly FJ, MacNeil MA, Brown SP, Masland RH. The diversity of ganglion cells in a mammalian retina. J Neurosci. 2002; 22(9):3831–3843. [PubMed: 11978858]

Rockhill RL, Euler T, Masland RH. Spatial order within but not between types of retinal neurons. Proc Natl Acad Sci U S A. 2000; 97(5):2303–2307. [PubMed: 10688875]

Rodieck RW. The density recovery profile: a method for the analysis of points in the plane applicable to retinal studies. Vis Neurosci. 1991; 6(2):95–111. [PubMed: 2049333]

Roska B, Molnar A, Werblin FS. Parallel processing in retinal ganglion cells: how integration of space-time patterns of excitation and inhibition form the spiking output. J Neurophysiol. 2006; 95(6):3810–3822. [PubMed: 16510780]

Roska B, Werblin F. Vertical interactions across ten parallel, stacked representations in the mammalian retina. Nature. 2001; 410(6828):583–587. [PubMed: 11279496]

Schmitz F, Königstorfer A, Südhof TC. RIBEYE, a component of synaptic ribbons: a protein's journey through evolution provides insight into synaptic ribbon function. Neuron. 2000; 28(3):857–872. [PubMed: 11163272]

Shepherd, GM. The synaptic organization of the brain. Shepherd, GM., editor. New York: Oxford University Press; 2003. p. 736

Shepherd GM, Raastad M. Axonal varicosity distributions along parallel fibers: a new angle on a cerebellar circuit. Cerebellum. 2003; 2(2):110–113. [PubMed: 12880178]

Shepherd GM, Raastad M, Andersen P. General and variable features of varicosity spacing along unmyelinated axons in the hippocampus and cerebellum. Proc Natl Acad Sci U S A. 2002; 99(9): 6340–6345. [PubMed: 11972022]

Sivyer B, Taylor WR, Vaney DI. Uniformity detector retinal ganglion cells fire complex spikes and receive only light-evoked inhibition. Proc Natl Acad Sci U S A. 2010; 107(12):5628–5633. [PubMed: 20212117]

Song S, Sjostrom PJ, Reigl M, Nelson S, Chklovskii DB. Highly nonrandom features of synaptic connectivity in local cortical circuits. PLoS Biol. 2005; 3(3):e68. [PubMed: 15737062]

Stevens JK, McGuire BA, Sterling P. Toward a functional architecture of the retina: serial reconstruction of adjacent ganglion cells. Science. 1980; 207(4428):317–319. [PubMed: 7350663]

Taylor WR, He S, Levick WR, Vaney DI. Dendritic computation of direction selectivity by retinal ganglion cells. Science. 2000; 289(5488):2347–2350. [PubMed: 11009420]

tom Dieck S, Altrock WD, Kessels MM, Qualmann B, Regus H, Brauner D, Fejtova A, Bracko O, Gundelfinger ED, Brandstätter JH. Molecular dissection of the photoreceptor ribbon synapse: physical interaction of Bassoon and RIBEYE is essential for the assembly of the ribbon complex. J Cell Biol. 2005; 168(5):825–836. [PubMed: 15728193]

Trexler EB, Li W, Mills SL, Massey SC. Coupling from AII amacrine cells to ON cone bipolar cells is bidirectional. J Comp Neurol. 2001; 437(4):408–422. [PubMed: 11503143]

Van Haesendonck E, Missotten L. Stratification and square pattern arrangements in the dorsal inner plexiform layer in the retina of Callionymus lyra L. J Ultrastruct Res. 1983; 83(3):296–302. [PubMed: 6876251]

Van Haesendonck E, Missotten L. Patterns of glutamate-like immunoreactive bipolar cell axons in the retina of the marine teleost, the dragonet. Vision Res. 1991; 31(3):451–462. [PubMed: 1688217]

Van Wyk M, Taylor WR, Vaney DI. Local edge detectors: a substrate for fine spatial vision at low temporal frequencies in rabbit retina. J Neurosci. 2006; 26(51):13250–13263. [PubMed: 17182775]

Wagner HJ. The connectivity of cones and cone horizontal cells in a mosaic-type teleost retina. Cell Tissue Res. 1976; 175(1):85–100. [PubMed: 1000600]

Wässle H. Parallel processing in the mammalian retina. Nat Rev Neurosci. 2004; 5(10):747–757. [PubMed: 15378035]

Wässle H, Boycott BB, Illing RB. Morphology and mosaic of on- and off-beta cells in the cat retina and some functional considerations. Proc R Soc Lond B Biol Sci. 1981; 212(1187):177–195. [PubMed: 6166013]

Wässle H, Puller C, Muller F, Haverkamp S. Cone contacts, mosaics, and territories of bipolar cells in the mouse retina. J Neurosci. 2009; 29(1):106–117. [PubMed: 19129389]

Wässle H, Riemann HJ. The mosaic of nerve cells in the mammalian retina. Proc R Soc Lond B Biol Sci. 1978; 200(1141):441–461. [PubMed: 26058]

Werblin F, Roska B, Balya D. Parallel processing in the mammalian retina: lateral and vertical interactions across stacked representations. Prog Brain Res. 2001; 131:229–238. [PubMed: 11420943]

Xu Y, Vasudeva V, Vardi N, Sterling P, Freed MA. Different types of ganglion cell share a synaptic pattern. J Comp Neurol. 2008; 507(6):1871–1878. [PubMed: 18271025]

Young RW. Cell differentiation in the retina of the mouse. Anat Rec. 1985; 212(2):199–205. [PubMed: 3842042]

Zhang J, Li W, Trexler EB, Massey SC. Confocal analysis of reciprocal feedback at rod bipolar terminals in the rabbit retina. J Neurosci. 2002; 22(24):10871–10882. [PubMed: 12486181]

Zheng JJ, Lee S, Zhou ZJ. A developmental switch in the excitability and function of the starburst network in the mammalian retina. Neuron. 2004; 44(5):851–864. [PubMed: 15572115]

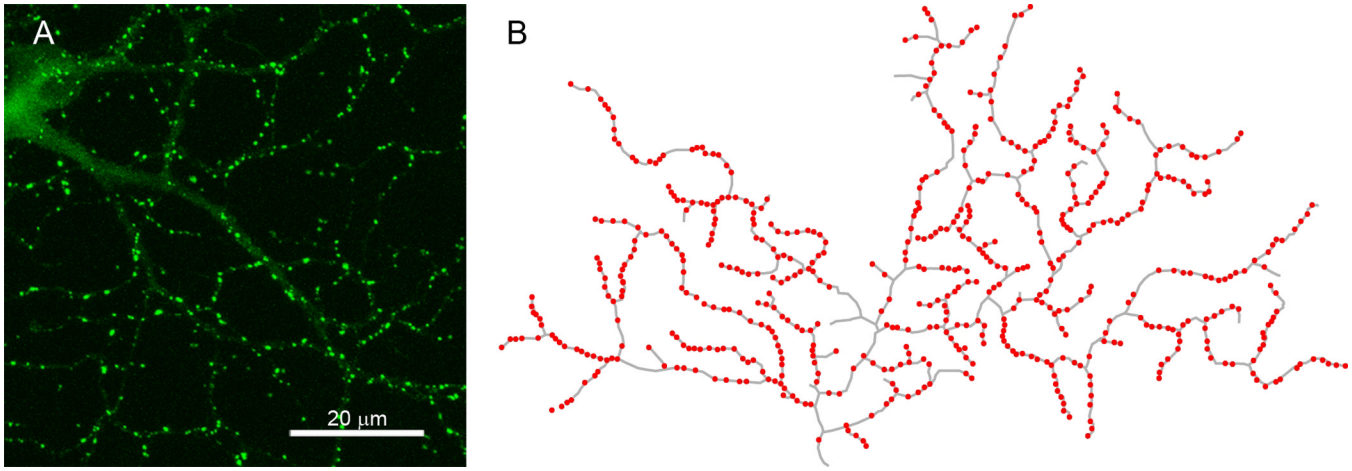

Figure 1.

(A) Expression of PSD95-GFP in dendrites of a retinal ganglion cell. The plasmid was introduced with a gene gun followed by 4 days in organ culture. (**B**) The pattern of excitatory inputs to a retinal ganglion cell. The cell was skeletonized by manual entry into the Neurolucida software package. The locations of the PSD95 puncta are given by orange dots.

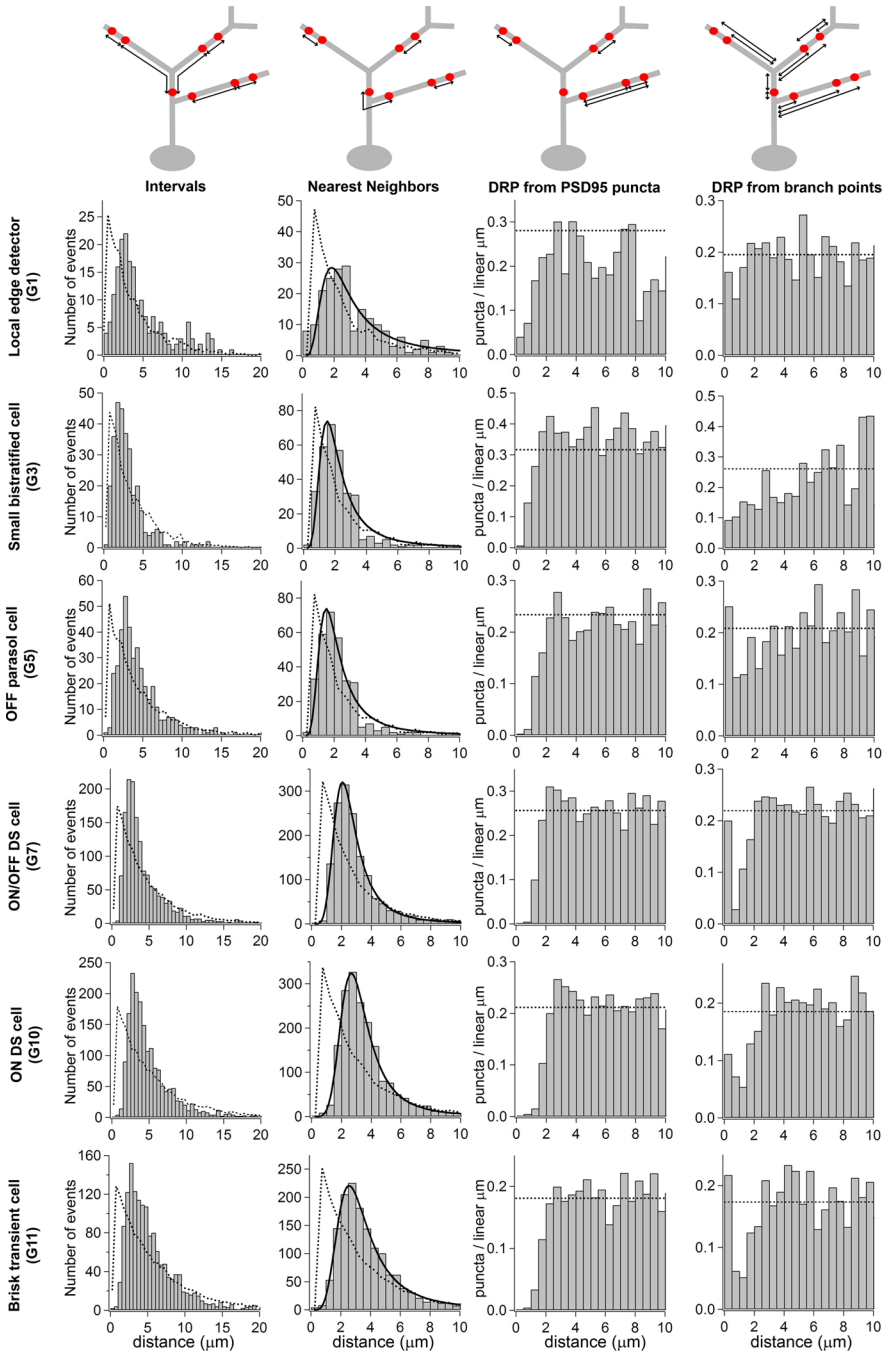

Figure 2.

The sites of excitatory input are non-randomly distributed along the dendrites. In all measurements the actual distribution of PSD95 puncta is compared with the distribution of the same number of puncta on that same dendritic structure at random (dotted lines). In the distribution of intervals, the nearest neighbor distances, and the spatial autocorrelation, there is always evidence of an “exclusion zone”: a zone around the reference element from which PSD95 puncta tend to be excluded. This appears in the total distribution of intervals as a greater than chance frequency of intervals at about 3.0 µm, and in the nearest neighbor analysis as a rightward shift in the distribution of intervals. These differences were statistically significant. For the OFF parasol, ON-OFF DS, ON DS, brisk transient, and

starburst cells the level of significance by the Kolmogorov-Smirnov test was $p < 0.0001$. For the small bistratified cell and local edge detectors the level was $p < 0.01$ or less. The exclusion zone can be directly visualized in the spatial autocorrelation (DRP) where a zone is seen near each punctum, from which PSD95 puncta tend to be excluded. In the DRP, the frequency of occurrence rises to an asymptote, at which point the spacing of events relative to the reference point is random. The distribution of puncta around branch points varied more among cell types. For the brisk transient, ON DS; ON-OFF DS, and OFF parasol cells, puncta could occur near branch points at about the level expected by chance. Immediately adjacent, however, the probability of a punctum was well below random – an exclusion zone was present. For the small bistratified cells and the local edge detectors, branch points had fewer puncta than expected by chance. As for the other cell types, the region surrounding the branch point was also poor in puncta – there was the same exclusion zone as for the other cells. (These were weak tendencies in the case of the local edge detectors, possibly related to their small size and dense branching pattern.)

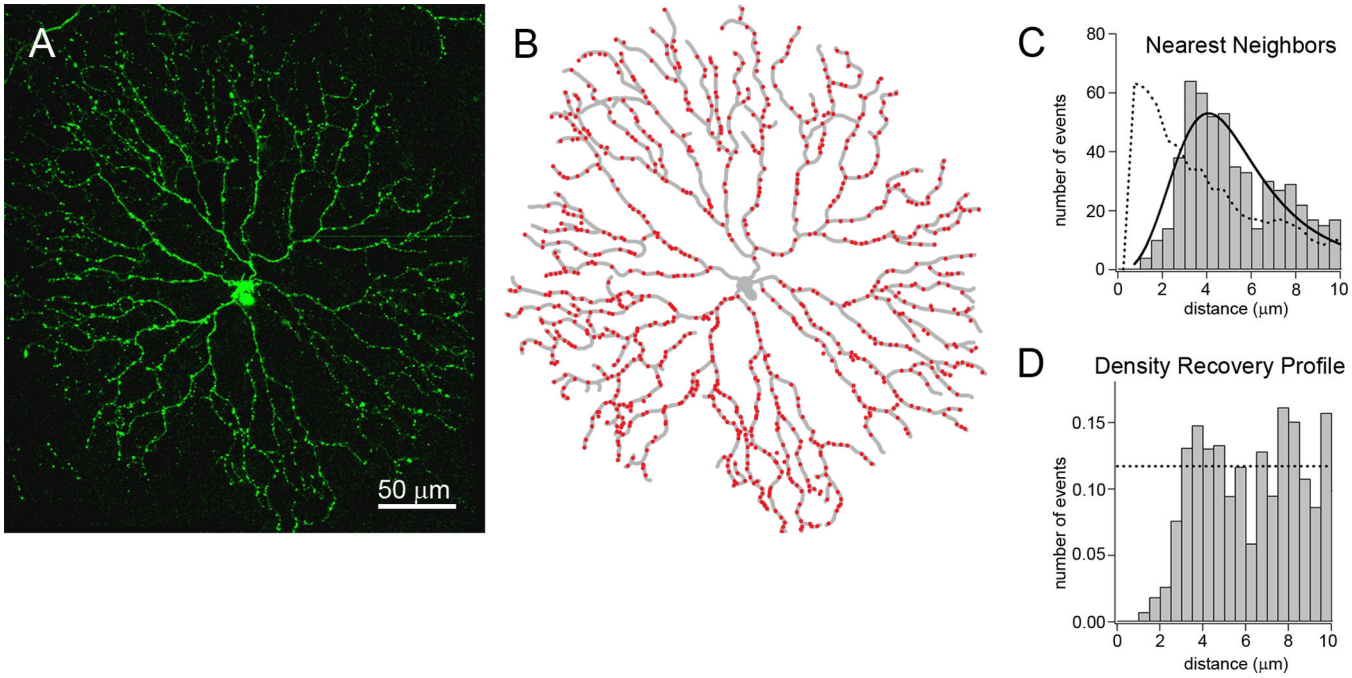

Figure 3.

The spacing of excitatory inputs to a starburst amacrine cell. **(A, B)** PSD95 puncta and their skeletonized representation. **(C)** Nearest neighbor distribution along the dendrites. **(D)** Spatial autocorrelation (DRP) of the puncta. The values at longer distances from the reference point are more variable than for the ganglion cells, because of the lower density of puncta between branch points, but the fundamental point – the exclusion zone – is quite clear. The method of measuring the spacing is the same as diagrammed in Figure 2.

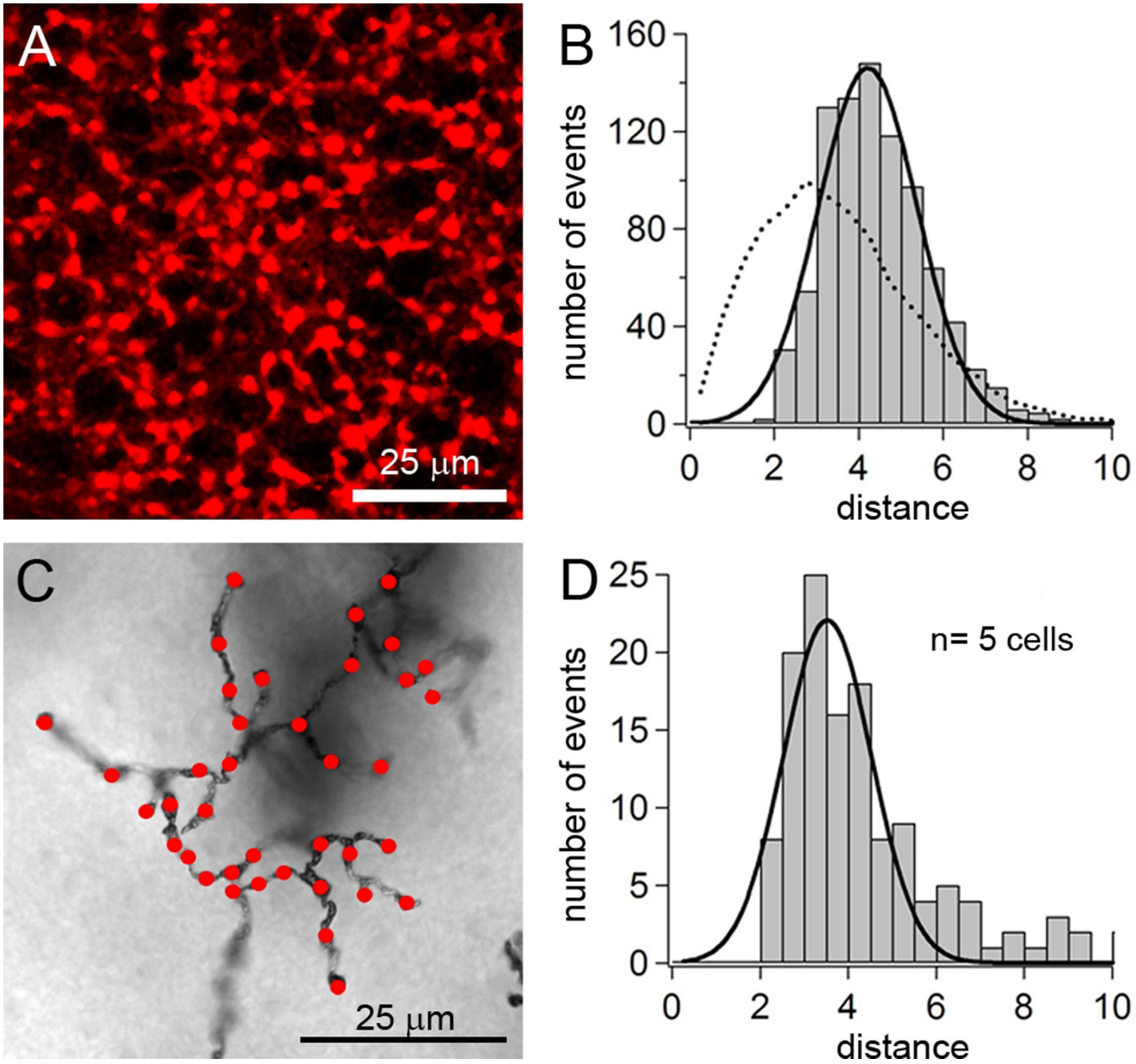

Figure 4.

The axonal varicosities of most types of bipolar cells are also regularly spaced. (**A**) CD15 stained mosaic of bipolar axons. Scale bar = 25 μm. **(B)** Nearest neighbor distribution (average of three 204 × 204 μm fields). Dotted line shows the distribution expected by chance, calculated from 10 samples of randomized distributions. The data are fitted by Gaussian curves. **(C)** An example of a Golgi-stained bipolar cell. This cell had dendrites stratifying at 20% depth of the inner plexiform layer, where the margin of the INL is taken as 0. **(D)** Nearest neighbor distributions for varicosities of 5 bipolar cells stratified at this depth. Shrinkage due to the Golgi-staining procedure and mounting was corrected by 30%.

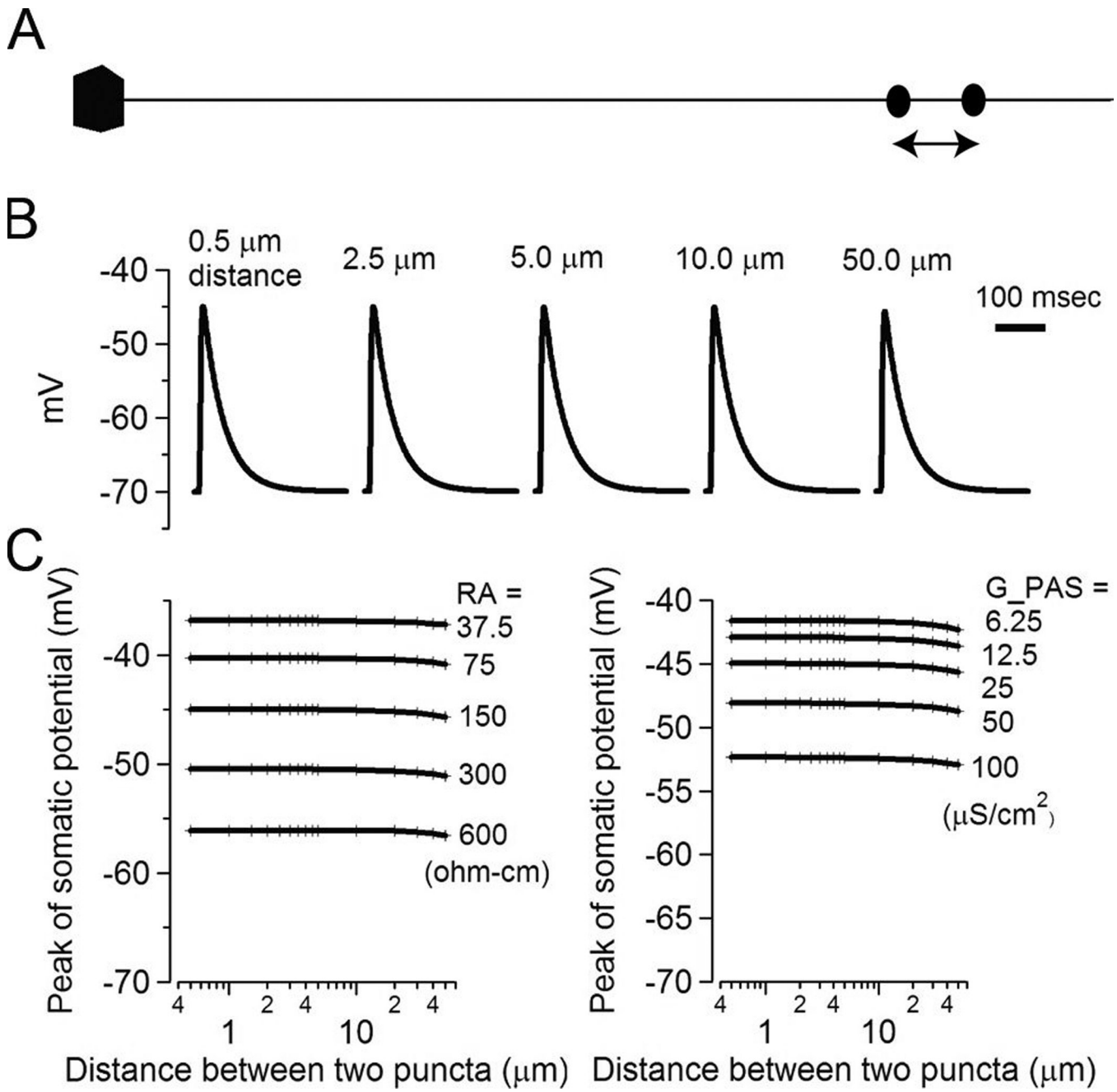

Figure 5.

Modeling: the spacing of synaptic input zones does not much affect their effectiveness at the soma. (**A**) A schematic neuron with a single dendrite containing only two excitatory synapses: one is located 200 μm from the soma and the second synapse had a variable position between 200 and 250 μm from the soma. (**B**) Somatic responses when two synapses were simultaneously stimulated. The distance between two synapses had little effect upon the response transmitted to the soma. (**C**) This remained the case for a wide range of membrane capacitance (g_pas) and intracellular resistance (RA).

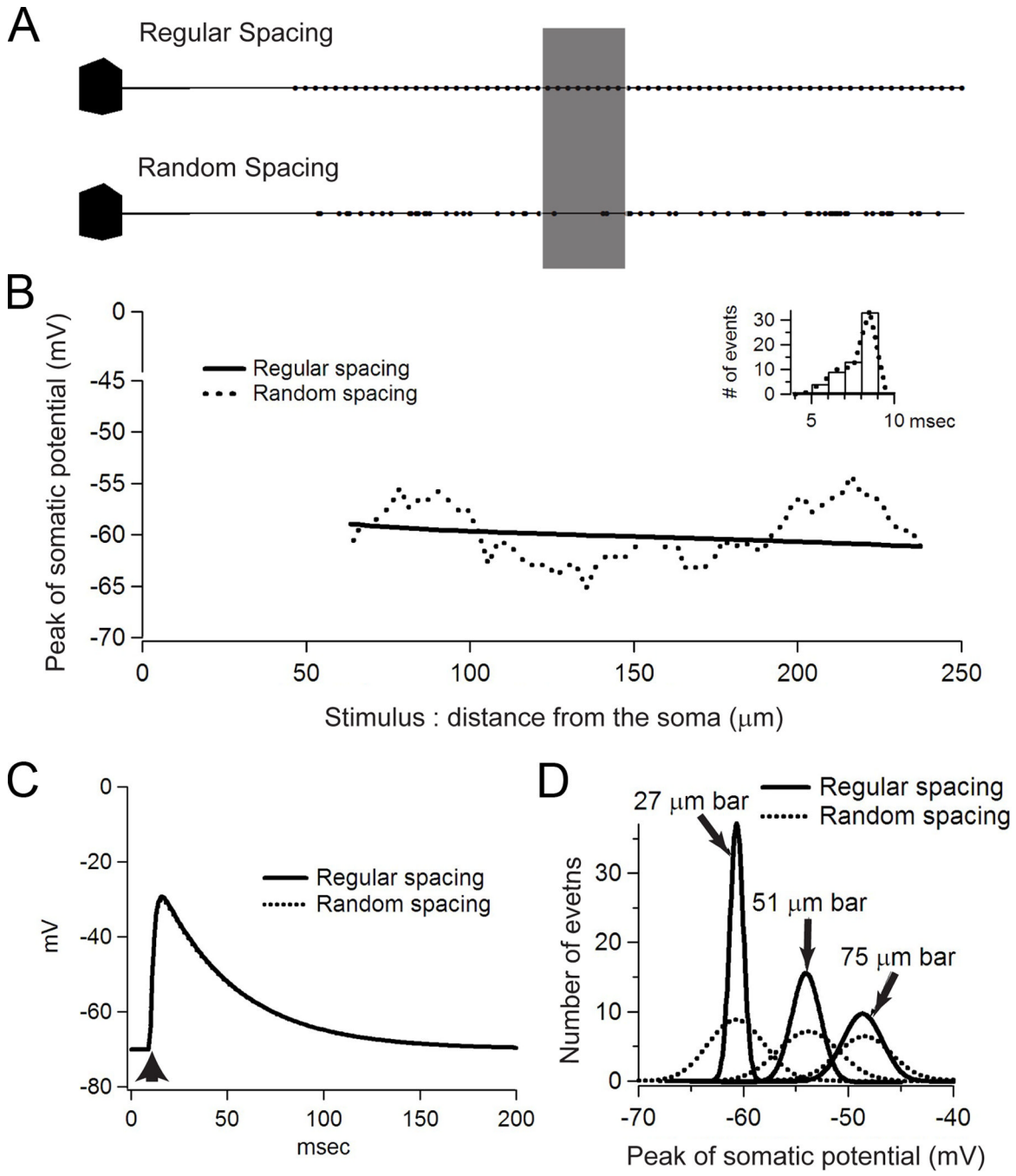

Figure 6.

In principle, regular spacing would make the detection of synaptic inputs more reliable. (**A**) A schematic neuron possessing only a single dendrite. A fixed number of synapses were distributed with regular 3 μm spacing or random spacing at the same average interval. A fixed size of stimulus (27, 51, and 75 μm width) was applied to the cell model at various locations. (**B**) The peak potential of somatic responses when the dendrite was stimulated by an input of 27 μm width. If the synaptic input sites were randomly located, the peak potential varied considerably, while regular spacing gave more consistent responses. Inset: Timing of the peaks was not different for regular spacing and random spacing. (**C**) When all of the synapses were simultaneously stimulated, there was no difference between regular

spacing and random spacing. (**D**) These histograms show the distribution of somatic peak potentials resulting from 27, 51 and 75 μm width stimulation, when the simulated neuron has synapses at regular (solid lines) and random (dotted lines) spacing. When the cells were stimulated by a 27 μm wide input, regular spacing gave a much less variable response, as indicated by the narrow width of the distribution of responses. However, the difference from a random distribution was far less for the 75 μm wide stimulation.

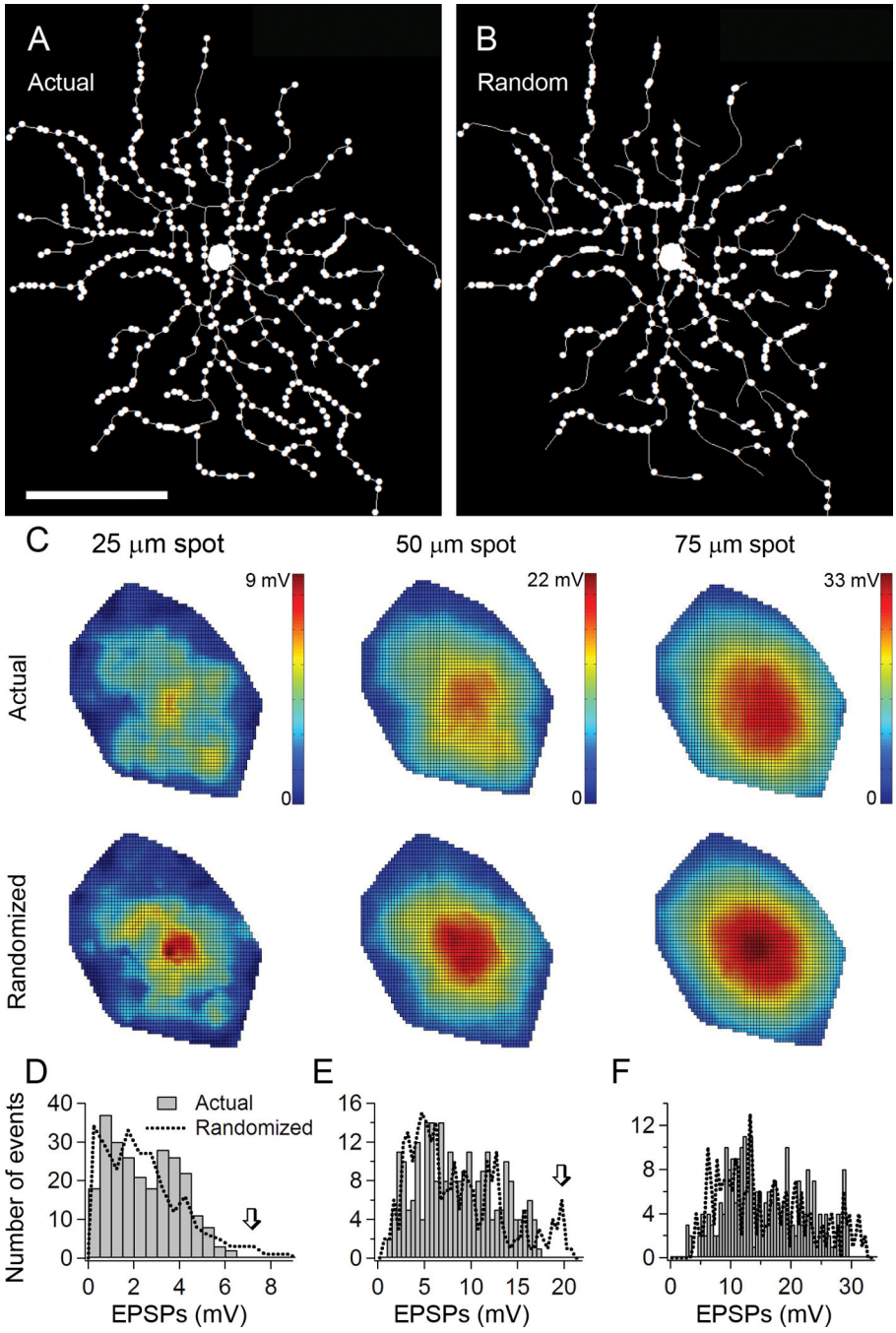

Figure 7.

For a more realistic cell, the space filling nature of the dendritic tree smooths the cell's responses to realistic inputs (i.e. inputs that have the size of the axonal arbors of cone bipolar cells.) (**A and B**) At the top, NeuroLucida tracings of the modeled ganglion cell are shown. In one case the cell had the actual spacing observed for the synapses (**A**). In the other, the same number of synapses were distributed at random (**B**). Assignment of synapses to the connecting vertical dendrites was prohibited, as is the case in the actual distribution of synapses. (**C**) A region of stimulation with a diameter of 25, 50 or 75 μm was presented at 250 random locations within the dendritic field and the somatic responses were recorded. (**D, E, and F**) The peak amplitudes were plotted in the locations of the centers of the spots

and contoured by the surface function of MatLab for the spot sizes of 25 μm (**D**), 50 μm (**E**), and 75 μm (**F**). The greatest difference between the two cases is a slightly greater number of hot spots (arrows in panels **D** and **E**) in the random case.

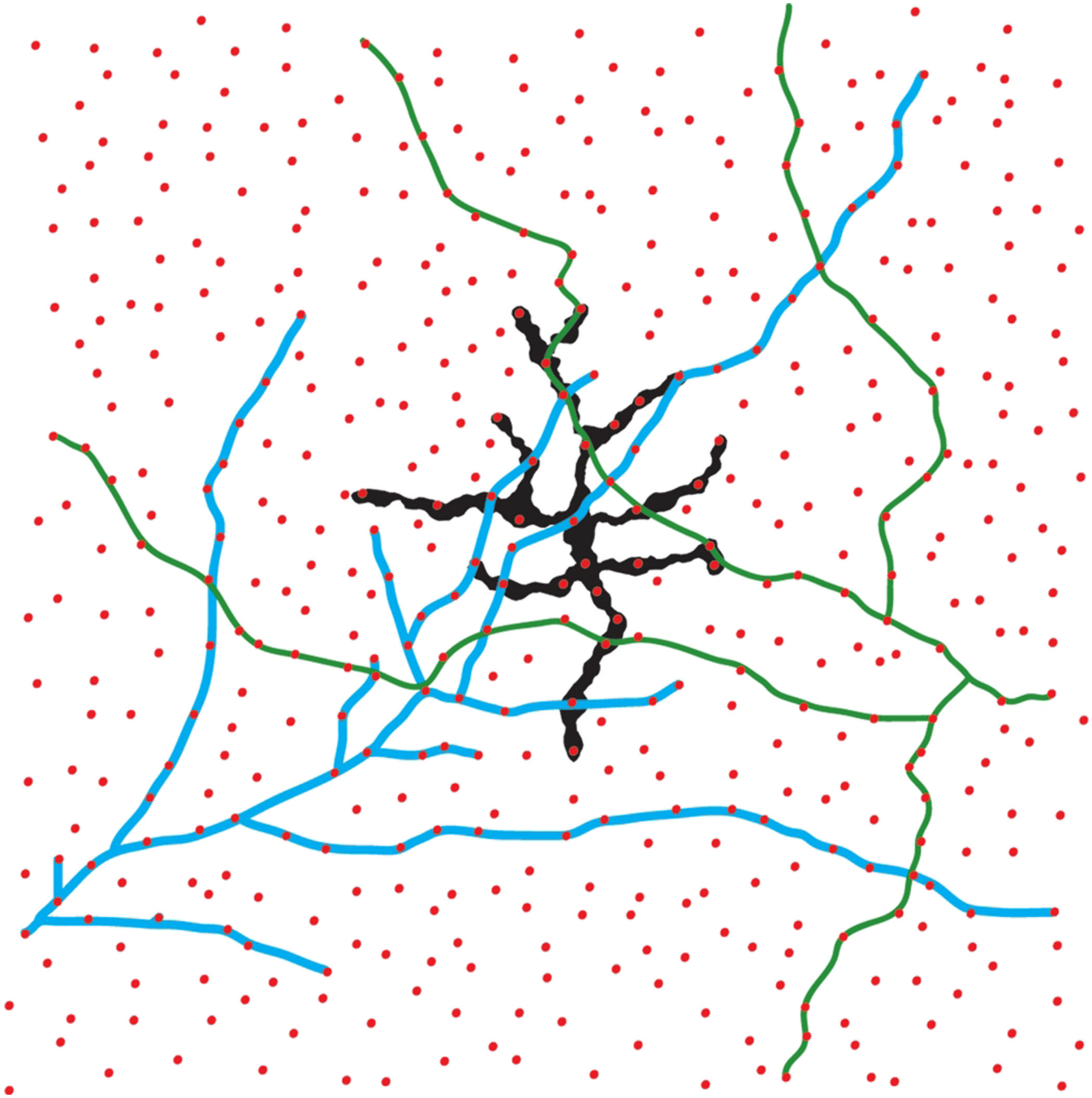

Figure 8.

The mosaic of excitatory contacts within the inner plexiform layer. The red dots represent the whole mosaic, as it would exist for a single type of stratified bipolar cell. An individual bipolar cell is shown in black, dendrites of a ganglion cell in blue, and dendrites of an amacrine cell in green. This is an attempt to synthesize the facts established here about the spacing of synapses in the three cell types – i.e. to represent the situation that needs to occur given the regularities of spacing described for the bipolar, ganglion and starburst cells. This illustration shows a case in which very few possible contacts between the three cell types are skipped. If contacts are skipped, longer intervals will appear in the DRP, but the

fundamental spacing module (i.e. the irreducible minimum exclusion zone in the DRP, which is determined by the mosaic of red dots in this schematic) will remain (Cook, 1996).

Table 1

Primary Antibodies used

Antigen	Immunogen	Manufacturer, host species, catalog number	Dilution used
CD15 (Lacto-N-fucopentatose III)	U-937 histiocytic cell line	BD Pharmingen (San Jose, CA), mouse monoclonal IgM, #559045	1 μg/ml
calbindin D-28k	mouse recombinant calbindin protein	Millipore, (Billerica, MA), rabbit polyclonal, #AB1778	1 μg/ml
CtBP2 (RIBEYE)	amino acids 361–445 of the mouse CtBP2 protein	BD Transduction Laboratories (San Jose, CA), mouse monoclonal IgG, #612044	2 μg/ml

Table 2

The Density of PSD95-GFP Puncta on Ganglion cells of Differing Morphological Types

Ganglion cell type		Number of PSD95 puncta	Dendritic field diameter (μm)	Total length of dendrites (μm)	Puncta / linear μm
Local Edge Detector	#1	187	86.86	1034.80	0.18
	#2	204	78.98	831.46	0.25
Small Bistratified	#1	316	104.91	1144.40	0.28
OFF Parasol	#1	406	156.39	1678.70	0.24
	#2	381	156.63	2050.30	0.19
ON-OFF DS	#1	1537	282.94	6707.30	0.23
	#2	565	126.16	2503.40	0.23
ON DS	#1	1845	531.87	9625.80	0.19
Brisk Transient	#1	1492	553.41	8470.30	0.18
	#2	1121	549.37	7732.60	0.15
$\bar{X}$					0.19

Table 3

Nearest Neighbor Spacing for the Axonal Varicosities of Bipolar Cells.

	IPL stratum	N	Number of varicosities	NND (μm)
Golgi-stained Cells	1	5 cells	129	3.59 ± 1.07
	2	7 cells	171	3.89 ± 1.27
	3	11 cells	312	3.73 ± 1.12
	4	10 cells	264	4.06 ± 1.35
CD15-stained fields	4	3 fields	875	4.22 ± 1.22
			854	4.10 ± 1.15
			904	4.30 ± 1.10
$\bar{X}$				3.98